



Transplantation of Human Adipose Stem Cells Using Acellular Human Amniotic Membrane Improves Angiogenesis in Injured Endometrial Tissue in a Rat Intrauterine Adhesion Model

Cell Transplantation
Volume 29: 1–11
© The Author(s) 2020
Article reuse guidelines:
sagepub.com/journals-permissions
DOI: 10.1177/0963689720952055
journals.sagepub.com/home/ctj


Xiao Han^{1,*}, Yuejiao Ma^{2,*}, Xin Lu², Weihong Li², Enlan Xia¹,
Tin-Chiu Li^{1,3}, Haiyan Zhang², and Xiaowu Huang¹ 

Abstract

Endometrial injury resulting in intrauterine adhesion is associated with extensive damage to the regenerative basal layer of the endometrium and represents a major therapeutic challenge. Human adipose stem cells (hASCs) hold promise for future clinical use in the individualized therapy of injured endometrial tissue. Here, we observed that the use of the acellular human amniotic membrane (AHAM) significantly increased the expression of angiogenic factors, including angiogenin (ANG) and vascular endothelial growth factor (VEGF), in hASCs *in vitro*. The three-dimensional engineered hASC-AHAM grafts significantly increased the endometrial receptivity, as increased endometrial thickness, greater numbers of endometrial glands, and higher protein levels of leukemia inhibitory factor were observed in injured endometrial tissue that was treated with these grafts compared to those detected in injured endometrial tissue that was treated with AHAM alone. In addition, the hASC-AHAM grafts significantly increased the vascular density in the injured endometrial tissue in rats, when transplanted into an injured uterine cavity. Using the EGFP⁺-hASC-AHAM grafts for transplantation, we confirmed that the hASCs maintained higher protein levels of ANG and VEGF in the injured uterine cavity *in vivo*. The results of this study suggest that the ability of the engineered hASC-AHAM grafts to repair injured endometrial tissue may be associated with their ability to promote angiogenesis through the upregulated expression of angiogenic factors in hASCs. These findings may support individualized stem cell-based therapy for endometrial disease using bioartificial grafts.

Keywords

intrauterine adhesion, stem cells, human amniotic membrane, VEGF, angiogenin

Introduction

Intrauterine adhesion (IUA), often known as Asherman's syndrome, is characterized by the aberrant adhesions within the uterus and/or cervix and is a major gynecological disease¹. Patients with IUA may present with menstrual abnormalities, infertility, recurrent miscarriage, and sometimes pelvic pain. Despite evidences showing that approximately 90% of IUA cases are caused by curettage or infection, especially after pregnancy, the pathogenesis of IUAs has not been fully elucidated². Currently, the treatment for IUAs is primarily based on the hysteroscopic lysis of adhesions, hormonal therapy to promote endometrial regeneration, and use of a physical barrier to prevent the

¹ Hysteroscopic Center, Fuxing Hospital, Capital Medical University, Beijing, China

² Department of Cell Biology, Municipal Laboratory for Liver Protection and Regulation of Regeneration, Capital Medical University, Beijing, China

³ Assisted Conception Unit, Department of Obstetrics and Gynecology, Chinese University of Hong Kong, Prince of Wales Hospital, Hong Kong, China

* Both the authors contributed equally to this article

Submitted: February 4, 2020. Revised: July 31, 2020. Accepted: August 2, 2020.

Corresponding Author:

Xiaowu Huang, Hysteroscopic Center, Fuxing Hospital, Capital Medical University, No. 20, Fuxingmenwai Avenue, Beijing 100038, China.
Email: hxiaowu_fxyy@126.com



Creative Commons Non Commercial CC BY-NC: This article is distributed under the terms of the Creative Commons Attribution-NonCommercial 4.0 License (<https://creativecommons.org/licenses/by-nc/4.0/>) which permits non-commercial use, reproduction and distribution of the work without further permission provided the original work is attributed as specified on the SAGE and Open Access pages (<https://us.sagepub.com/en-us/nam/open-access-at-sage>).

recurrence of adhesion³. Endometrial stem cells, which have been shown to promote the regeneration of damaged endometrium, appear to do not hold promise for use in refractory cases^{4–6}.

Recent studies have shown that transplantation of human embryonic stem cells⁷, bone marrow mesenchymal stem cells^{8,9}, human umbilical cord mesenchymal stem cells¹⁰, menstrual blood-derived stromal cells¹¹, human endometrial mesenchymal stem cells¹², and human adipose stem cells (hASCs)^{13,14} has beneficial effects on endometrial repair and regeneration. Among these various types of stem cells, hASCs have been considered particularly suitable for clinical individualized regenerative therapies because they are more readily available and exhibit substantial plasticity¹⁵.

At present, the treatment of endometrial injury by stem cells is mainly performed through the intravenous or intrauterine routes. However, increasing evidence has shown that treatment with healthy stem cells through these routes may hinder engraftment because most diseased endometria have altered architectures due to fibrosis and cirrhosis. New developments in engineering technology have introduced functional grafts that combine stem cells with biomaterials, such as hydrogels, hyaluronic acid, and nanostructured lipid carriers¹⁶. Another ideal scaffold with the appropriate microarchitecture, extracellular matrix components, and lower immunogenicity is acellular human amniotic membrane (AHAM), which has been used as a scaffold for hepatocyte-like cells derived from hASCs¹⁷. Functional AHAM-hepatocytes grafts integrated in the livers of mice have been shown to decrease acute liver injury, suggesting that AHAMs may be more suitable for stem cell transplantation in endometrial regeneration.

In this study, we aimed to determine the morphology and function of hASCs with AHAMs and to investigate the ability and the underlying mechanism of the hASC-AHAM grafts in the repair of injured endometrial tissue in a rat model.

Materials and Methods

Cell Isolation and Culture

hASCs from four different donors were developed, according to our previous report¹⁸. Cells from passage six were used in this study. Briefly, hASCs were isolated from subcutaneous adipose tissue from nondiabetic donors aged 39–53 years with informed patient consent and under the approval of the Ethics Committee of Capital Medical University (Beijing, China). The adipose tissue was minced into pieces, washed twice in phosphate-buffered saline (PBS, pH 7.2) with 5% penicillin–streptomycin, and then digested with 0.075% type I collagenase (Invitrogen, Grand Island, NY, USA) for 180 min at 37°C with gentle shaking. The digests were then centrifuged at 1,500 rpm for 5 min at 4°C. The pellets were washed twice with PBS, filtered using a cell strainer (BD Biosciences, San Jose, CA, USA), and

resuspended in Dulbecco's Modified Eagle Medium/Nutrient Mixture F-12 (DMEM/F-12; Invitrogen) supplemented with 10% fetal bovine serum mesenchyme stem cell screened (Hyclone, Logan, UT, USA). The cells were incubated in a humidified incubator at 37°C with 5% CO₂. Once 90% confluence was achieved, the cells were harvested using 0.05% trypsin–0.02% ethylenediaminetetraacetic acid (EDTA; Sigma-Aldrich, St. Louis, MO, USA) solution and resuspended at a density of 3×10^5 /ml.

Lentiviral-stable Transfection of hASCs

When the cells reached 80%–90% confluence, the medium was replaced with fresh complete medium supplemented with concentrated lentiviral vectors harboring pLV (Exp)-EGFP: T2A: Puro-Null (Cyagen Biosciences, Guangzhou, China) with 5 µg/ml polybrene (Solarbio, Beijing, China) for 24 h. Then, the cells were seeded into a new plate for selection using 1.0 µg/ml puromycin (Solarbio). After 7 days of screening, the medium was replaced with complete medium without puromycin, and cultivation was continued. The transduction results were evaluated using an inverted fluorescence microscope (Olympus, Tokyo, Japan).

Development of a Rat IUA Model

Sprague–Dawley female rats (6–8 weeks, 200–220 g) received care according to the Capital Medical University guidelines. The rats were injected with a single intraperitoneal dose of pregnant mare serum gonadotropin (ShuSheng, Ningbo, China) 48 h prior to the experiments.

The IUAs were developed according to our previous report^{14,19,20}. Briefly, the uterine horns of the rats ($n = 3$) were clipped with vascular clips and injured with 0.3–0.5 ml of 95% ethanol (vol/vol, each rat). The clips were removed after 5 min, and the horns were flushed with saline to dilute and remove any residual ethanol. Normal uterine horns ($n = 3$) were used as controls. Histological analysis of endometrial tissues was conducted by serial tissue sectioning and staining with hematoxylin and eosin (H&E), the endometrial thickness was measured, and the number of endometrial glands was counted.

Preparation of AHAM

AHAM was prepared as previously described^{17,21}. The HAM was obtained from a cesarean section operation at 37–40 weeks of pregnancy with informed patient consent and under the approval of the Ethics Committee of Capital Medical University. The ethics approval number is “2015SY72.” The donors age ranges from 25 to 35, with no history of membrane rupture, endometritis, meconium obstruction, HIV-1/2, hepatitis B, hepatitis C, human T-cell lymphovirus, syphilis, cytomegalovirus, and tuberculosis.

To prepare the AHAM, the HAM was peeled from the placenta, rinsed extensively in sterile PBS containing 200 U/

ml penicillin, 200 µg/ml streptomycin, and cut into approximately 5 cm × 5 cm pieces, which were placed in dishes with the amniotic epithelial layer face up. The AHAM pieces were incubated in 0.25% trypsin–0.38% EDTA for 30 min twice at 37°C, followed by rinsing in sterile PBS and dehydration in glycerol for 48 h; the glycerol was changed every day. Next, the fresh AHAM pieces were placed in dishes with a 1:1 mixture of glycerol and 0.5% chondroitin sulfate (Sigma–Aldrich) in MEM-NEAA (Gibco, Carlsbad, CA, USA) and stored at –80°C for several months. The AHAM tissue from three donors was used in this experiment.

Twenty-four hours before cell seeding, the cryopreserved AHAM was cut into approximately 0.5 cm × 0.5 cm pieces, rehydrated with sterile PBS twice for 30 min at 37°C, and then spread into 48-well cell culture plates with the basement membrane face up and cultured with DMEM/F-12 (Invitrogen) medium for at least 12 h.

Transplantation of the AHAM and hASC-AHAM Grafts

For examination or transplantation, EGFP⁺-hASC were seeded on the AHAM graft at a density of $1 \times 10^5/\text{cm}^2$. After 3 days of culture, EGFP⁺-hASC-AHAM could be used for experiments. hASCs were seeded on collagen type I (COLL I; Invitrogen) coated 48-well cell culture plates at the same density of $1 \times 10^5/\text{cm}^2$ as a control group for the *in vitro* experiment.

After 10 days of endometrial injury generation, the normal rats (four uterine horns) were used as a control group, and the rats with IUAs were randomly assigned to three groups (Supplemental Fig. S1), including an IUA group (six uterine horns), an IUA treated with AHAM group (IUA-AHAM, six uterine horns were transplanted, and each uterine horn included two pieces of AHAM tissue), and an IUA treated with hASC-AHAM group (IUA-hASC-AHAM, six uterine horns were transplanted, and each uterine horn included two pieces of AHAM containing 1×10^5 cells). The AHAM or hASC-AHAM was transplanted into the uterine cavity of rats without suture. The rats were injected with cyclosporine A (Solarbio) at 0.1 ml/day 24 h prior to experiments until they were sacrificed. The rats were injected with 160,000 units/day of penicillin for 3 days after transplantation of AHAM or hASC-AHAM and were sacrificed at day 15 after implantation.

Real-time Reverse Transcription Polymerase Chain Reaction

The hASCs were detached from the AHAM graft using 0.25% trypsin–0.02% EDTA solution for 3 min at 37°C, or from the COLL I using 0.05% trypsin–0.02% EDTA solution for 3 min at 37°C. And then the total cellular RNA was extracted from 2×10^5 cells with the RNeasy Mini Kit (QIAGEN, Hilden, Germany) according to the manufacturer's instructions. For polymerase chain reaction (PCR) analysis, 300 ng RNA was reverse transcribed to cDNA using

Superscript III reverse transcriptase and random hexamer primers (Invitrogen). Real-time PCR analysis was performed on an ABI Prism 7300 Sequence Detection System using the SYBR Green PCR Master Mix (Applied Biosystems, Foster City, CA, USA). The reaction consisted of 10 µl SYBR Green PCR Master Mix, 1 µl of a 5 µM mix of forward and reverse primers, 8 µl water, and 1 µl template cDNA in a total volume of 20 µl. Cycling was performed using the default conditions of the ABI 7300 SDS Software 1.3.1 (Applied Biosystems). The relative expression of each gene was normalized against 18 S rRNA. Data are presented as the mean ± standard deviation (SD). The primers are as follows: vascular endothelial growth factor (VEGF), forward: CTTGCCTTGCTGCTCTACCT and reverse: TTCGTGATGATTCTGCCCTC; ANG, forward: TGTTGTTGGTCTTCGTGCTG and reverse: TGATGTC TTTGCAGGGTGAG; and 18 S, forward: GTAACCCGTT-GAACCCATT and reverse: CCATCCAATCGGTAG TAGCG.

Histochemistry and Immunohistochemistry

For histological preparation, parts of the uteri were fixed with 10% formalin for 24 h, dehydrated with graded alcohols, and embedded in paraffin. The embedded tissues were then consecutively sliced into 5 µm thick sections and routinely stained with H&E. After H&E staining, the number of glands and the endometrial thickness were recorded in detail. The microscope magnifies the field of view by 200 times, at least five fields in each image and three images for each sample were randomly selected for counting, then calculated the average value.

Parts of the uterine horns were embedded in optimal cutting temperature compound (Sakura Finetek USA, Inc., Torrance, CA, USA) for 15 min at –20°C and then sliced using a frozen section preparation instrument Cryostat (Leica Microsystems, Inc., Buffalo Grove, IL, USA) to generate frozen sections (10 µm).

For immunohistochemistry, the transverse paraffin sections were deparaffinized and rehydrated. Then, the tissue sections were boiled at 110–120°C for 2 min for heat-induced antigen retrieval. After that the sections were incubated in 3% H₂O₂ for 10 min at room temperature. Subsequently, the samples were incubated with the primary antibodies, including leukemia inhibitory factor (LIF) (1:175; Biorbyt, Cambridge, UK) and CD34 (1:7,000; Abcam, Cambridge, UK) at 4°C overnight. The sections were then incubated with a tagged goat anti-mouse secondary antibody (Zhongshan, Beijing, China) for 20 min at room temperature. The DAB color reagent kit (Zhongshan) was used for color development, and the positive cells showed a brown color. The sections were imaged under a Leica microscope, and LIF expression was semi-quantitatively analyzed using the immunohistochemical score method (H-score). For the CD34-stained sections, we used 100 µm as the unit length. Measure the endometrial area of the submucosa of the uterine cross-section of a unit length of thickness, and count the

number of blood vessels in this range. Subsequently, the blood vessel density was calculated. The counting work was completed by two experimenters, each sample calculated three slices, and the average value was calculated.

Frozen tissue sections were incubated in 3% H₂O₂ for 5 min in a light-protected chamber at room temperature. Subsequently, the samples were incubated with primary antibodies, including VEGF (1:100; Proteintech, Chicago, IL, USA) and angiogenin (ANG; 1:75; Proteintech) at 4°C overnight. Following three 5-min washes in PBS with gentle agitation, the samples were incubated with an Alexa Fluor-conjugated secondary antibody (1:500; Invitrogen) for 1 h at 37°C in a light-protected chamber. The nuclei were counterstained with 4',6-diamidino-2-phenylindole (DAPI; Sigma-Aldrich). The relative optical density ANG and VEGF were calculated using ImageJ software. ImageJ was used to set positive area as the threshold and remove the influence of background signals. Pictures were converted into bitmap as a binary color (color = 1, no color = 0). The value of the calibration or scale was adjusted. The threshold was adjusted to separate the red in the picture from the background. Then, the area and cumulative absorbance of the selected area are obtained, and the optical density of the selected area is calculated.

Scanning Electron Microscopy

For scanning electron microscopy (SEM) analysis, the samples were fixed in 2.5% glutaraldehyde for 24 h at 4°C. Then the specimens were rinsed several times in 0.1 M phosphate buffer, fixed in 4% osmium phosphate-buffered solution, dehydrated in an acetone solution in distilled water at increasing concentrations, and kept in 100% acetone. Then the samples were dried in a critical point drier with carbon dioxide, mounted and coated with gold, and examined by SEM (Hitachi Limited, Tokyo, Japan).

Statistical Analysis

The statistical analyses were performed using the Statistical Package of Social Science 20.0 (IBM Corporation, New York, NY, USA). The data were expressed as mean \pm SD. The Student's *t*-test was used to compare groups. A *P* value of <0.05 was considered to be statistically significant.

Results

AHAM Promotes the Expression of Angiogenic Factors in hASCs

According to our previous report, the homogenous population of hASCs characterized by a high level of CD73, CD90, and CD105 express the pluripotent transcription factors OCT4, SOX2, NANOG, and SALL4¹⁸. And after decellularization and cryopreservation, AHAM retains the natural structure and composition of the HAM matrix, including the smooth and dense collagen substrate surface and the network

structure of collagen fibers and matrix. Collagen type I and fibronectin staining were observed in the basement membrane and in the compact layer of the AHAM, and the distribution of collagen type IV and laminin was primarily in the surface of the basement membrane and appeared to be intact in a linear pattern¹⁷.

To determine the morphology and function of hASCs with AHAM, the hASCs were seeded on COLL I-coated cell culture plates and on AHAM. The morphology of the hASCs was then observed via phase-contrast microscopy. By 72 h, the cells cultured on COLL I exhibited a typical hASCs morphology with a fibroblast-like shape, whereas those cultured on the AHAM aggregated into clusters, and curling of the amniotic membrane was observed. In addition, the histochemical results showed that the cells cultured on the AHAM appeared markedly long and thin, with observable edges and protrusions (Fig. 1A).

To suggest the functional activity of the hASC-AHAM graft, the differences in the expression of angiogenic factors, including ANG and VEGF, were assessed between the cells cultured on COLL I-coated substrate and the AHAM graft. Real-time reverse transcription polymerase chain reaction analyses showed that the mRNA levels of ANG and VEGF in the cells cultured on the AHAM were significantly higher than those observed in the cells cultured on COLL I (Fig. 1B). Furthermore, the immunohistochemical staining results showed that the cells cultured on the AHAM exhibited significant staining for ANG (Fig. 1C) and VEGF (Fig. 1D) compared with the cells on COLL I-coated plates (left panel is 2D-culture versus right panel is 3D-culture, and the cells cultured under 3D conditions are in a natural state rather than a flat state, so the cross-section looks smaller than cells under 2D-culture). The mean optical density results showed that the protein levels of ANG and VEGF in the cells cultured on the AHAM were significantly higher than those observed in the cells cultured on COLL I (Fig. 1E). These results were consistent with the morphological observations, indicating that AHAM has good compatibility with hASCs and promotes the expression of angiogenic factors in these cells.

Rat IUA Model with Ethanol Injury

To construct an animal model of IUA, the endometrium of rats was injured with ethanol. Ten days after the initiation injury, the properties of the rat endometria were determined via H&E staining. Compared with the normal group, the uterine cavities of rats in the ethanol-injured group appeared closed with the presence of IUAs (Supplemental Fig. S2). The endometrial thickness in the injury group ($122.7 \pm 9.6 \mu\text{m}$) was significantly thinner than that observed in the normal group ($516.0 \pm 11.6 \mu\text{m}$), and the number of endometrial glands per section in the injury group (2.5 ± 1.9) was significantly fewer than that observed in the normal group (15.3 ± 1.3) (Supplemental Fig. S2C). The results showed that the IUA model was successfully established with ethanol injury.

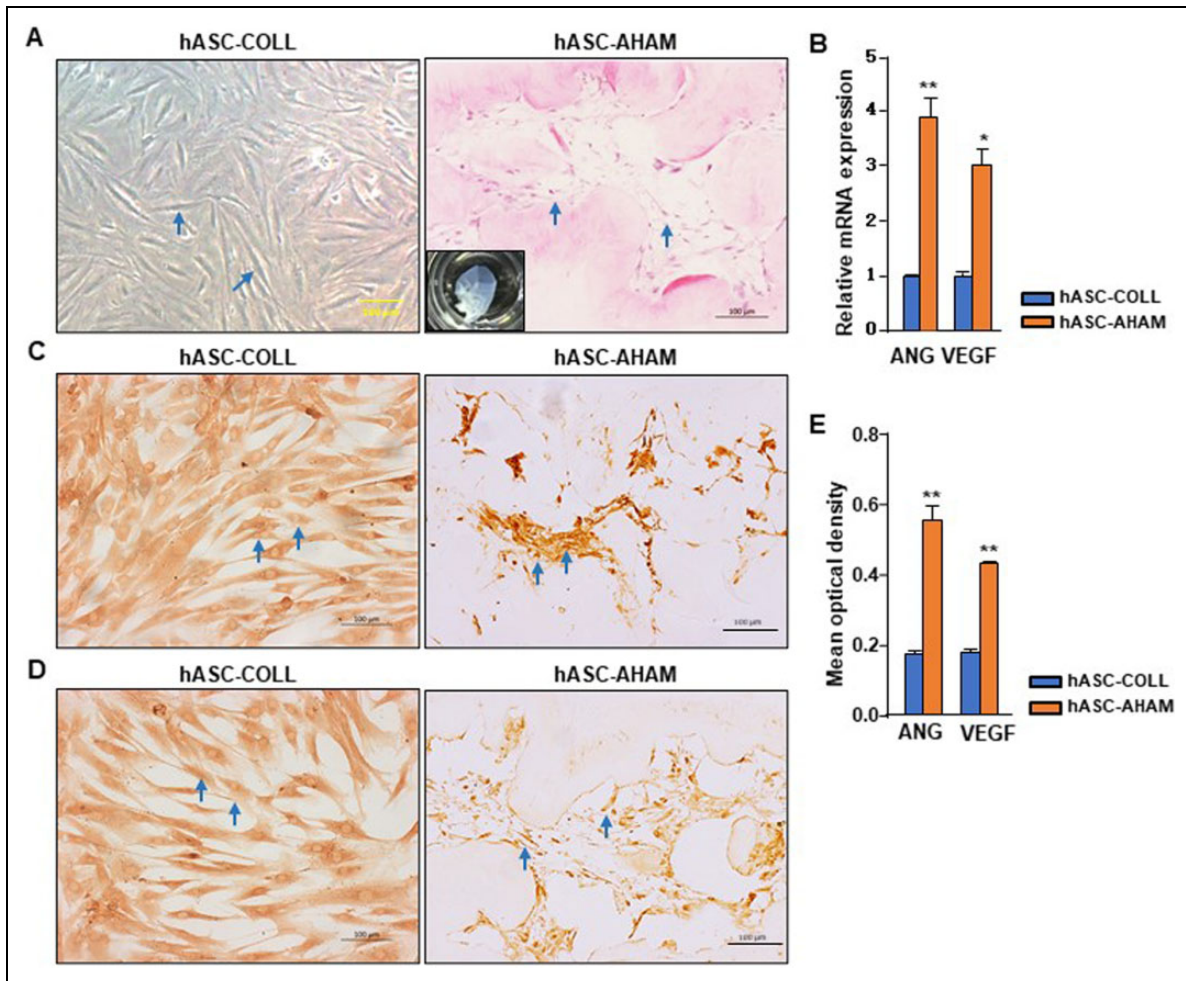


Figure 1. The morphology and expression of angiogenic factors in hASC-COLL and hASC-AHAM grafts. (A) The hASCs cultured on the COLL I-coated cell culture plates and the hASC-AHAM grafts were determined by H&E staining and observed by microscopy. The general appearance of the hASC-AHAM grafts cultured for 72 h is also shown. (B) Relative mRNA levels of ANG and VEGF in the hASC-COLL and hASC-AHAM grafts were determined by real-time RT-PCR. Relative protein levels of ANG (C) and VEGF (D) in the hASC-COLL and hASC-AHAM grafts were determined by immunohistochemical staining. (E) Protein levels of ANG and VEGF in the hASC-COLL and hASC-AHAM grafts were measured by determining the mean optical density. Significance compared to the hASC-COLL group. Blue arrows indicate the hASCs. AHAM: acellular human amniotic membrane; ANG: angiogenin; hASC: human adipose stem cell; hASC-AHAM: hASCs cultured in AHAM; hASC-COLL: hASCs cultured in COLL I-coated plates; H&E: hematoxylin and eosin; RT-PCR: reverse transcription polymerase chain reaction; VEGF: vascular endothelial growth factor.

hASC-AHAM Grafts Promote Functional Repair of the Injured Endometrium

To evaluate the ability of the hASC-AHAM grafts to repair injured endometrial tissue, the AHAM and hASC-AHAM grafts were transplanted into the injured endometria of rats. Uninjured (control) and IUA without transplantation were regarded as the positive and negative controls, respectively. SEM, histological, and immunohistochemical analyses were performed 15 days after transplantation to assess the engraftment of the transplanted AHAM or hASC-AHAM grafts. As shown in Fig. 2, a large amount of fibrous tissue appeared in the IUA group compared with that observed in the control group. In the IUA-AHAM group, small amounts of fibrous

tissue were observed, while the IUA-hASC-AHAM group had no obvious fibrous tissue, and was similar to the appearance of endometria in the control group.

The results of histological analyses showed that the mean endometrial thickness was $528.3 \pm 12.2 \mu\text{m}$ in the control group, $138.1 \pm 12.2 \mu\text{m}$ in the IUA group, $265.8 \pm 46.8 \mu\text{m}$ in the IUA-AHAM group, and $462.5 \pm 27.0 \mu\text{m}$ in the IUA-hASC-AHAM group. The endometrial thickness in the IUA-hASC-AHAM group was significantly greater than that observed in the IUA and IUA-AHAM groups, whereas that observed in the IUA-hASC-AHAM group was significantly thinner than in the control group (Fig. 3A, B). Furthermore, analyses of the numbers of glands showed that the mean number of endometrial glands per section was 15.3 ± 1.3

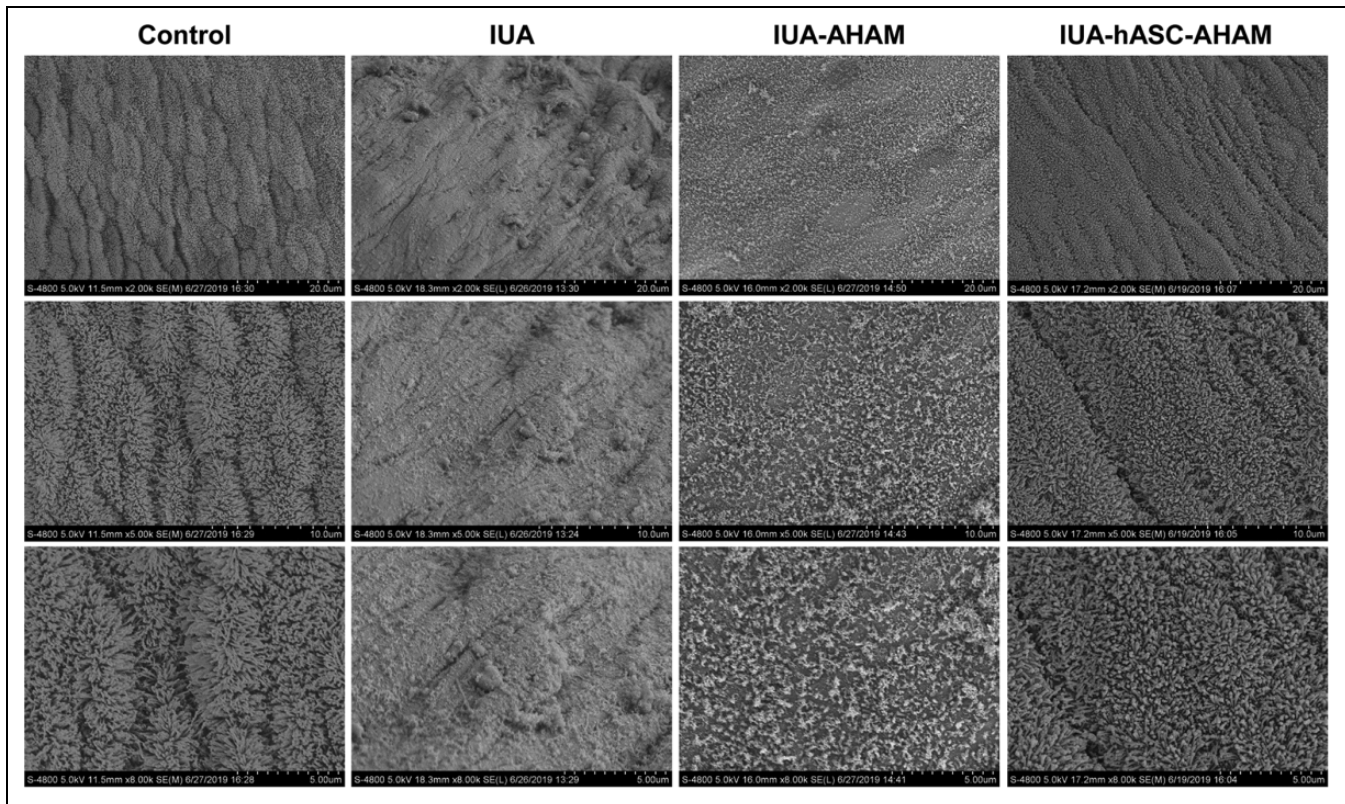


Figure 2. Histological analyses via scanning electron microscopy. The morphology and structure of the control, IUA, IUA-AHAM, and IUA-hASC-AHAM groups were determined using SEM. AHAM: acellular human amniotic membrane; hASC: human adipose stem cell; IUA: intrauterine adhesion; IUA-AHAM: IUA treated with AHAM; IUA-hASC-AHAM: IUA treated with hASC-AHAM.

in the control group, 2.5 ± 1.9 in the IUA group, 5.5 ± 3.1 in the IUA-AHAM group, and 11.0 ± 1.2 in the IUA-hASC-AHAM group. The number of glands observed in the IUA-hASC-AHAM group increased after the hASC-AHAM treatment compared with that observed in the IUA and IUA-AHAM groups (Fig. 3A, C).

To assess endometrial receptivity, the expression of LIF was evaluated in each group. The results showed that the mean H-score of LIF expression was 2.40 ± 0.75 in the control group, 2.04 ± 0.12 in the IUA group, 2.13 ± 0.10 in the IUA-AHAM group, and 2.32 ± 0.72 in the IUA-hASC-AHAM group. In addition, the IUA-hASC-AHAM group had significantly higher LIF expression levels than those observed in the IUA and IUA-AHAM groups ($P < 0.01$; $P < 0.01$) (Fig. 3D, E).

hASC-AHAM Grafts Promote Angiogenesis in the Injured Endometrium

To measure the vascular density in the injured endometrial tissue, the expression of CD34 was evaluated in each group. The results showed that the staining density of CD34 was 2.50 ± 0.17 in the control group, 0.51 ± 0.07 in the IUA group, 0.84 ± 0.02 in the IUA-AHAM group, and 1.69 ± 0.25 in the IUA-hASC-AHAM group. A significantly higher

staining density of CD34 was observed in the IUA-hASC-AHAM group than that in the IUA and IUA-AHAM groups (Fig. 4A, B). These results suggested that the hASC-AHAM grafts promoted highly efficient structural and functional repair of injured endometrial tissue *in vivo*.

To investigate the mechanism by which hASCs function to promote endometrial repair, EGFP⁺-hASCs were used in transplantation assays. The results showed that the EGFP⁺-hASCs were presented in the injury uterine cavity at day 15 after transplantation (Supplemental Fig. S3).

The fluorescence microscopy results verified that the EGFP⁺-hASCs present in the injured endometrium were positively stained with VEGF and ANG (Fig. 4C). These results indicate that the expression of VEGF and ANG in hASCs may play a role in repairing damaged endometrial tissue.

Taken together, these results suggested that hASC-AHAM grafts significantly increased the angiogenic factors in hASCs than that observed under the monolayer culture conditions.

Discussion

In this study, we observed that: (i) hASCs function well with AHAM grafts, which can create a feasible three-dimensional growth environment and increase the expression of VEGF

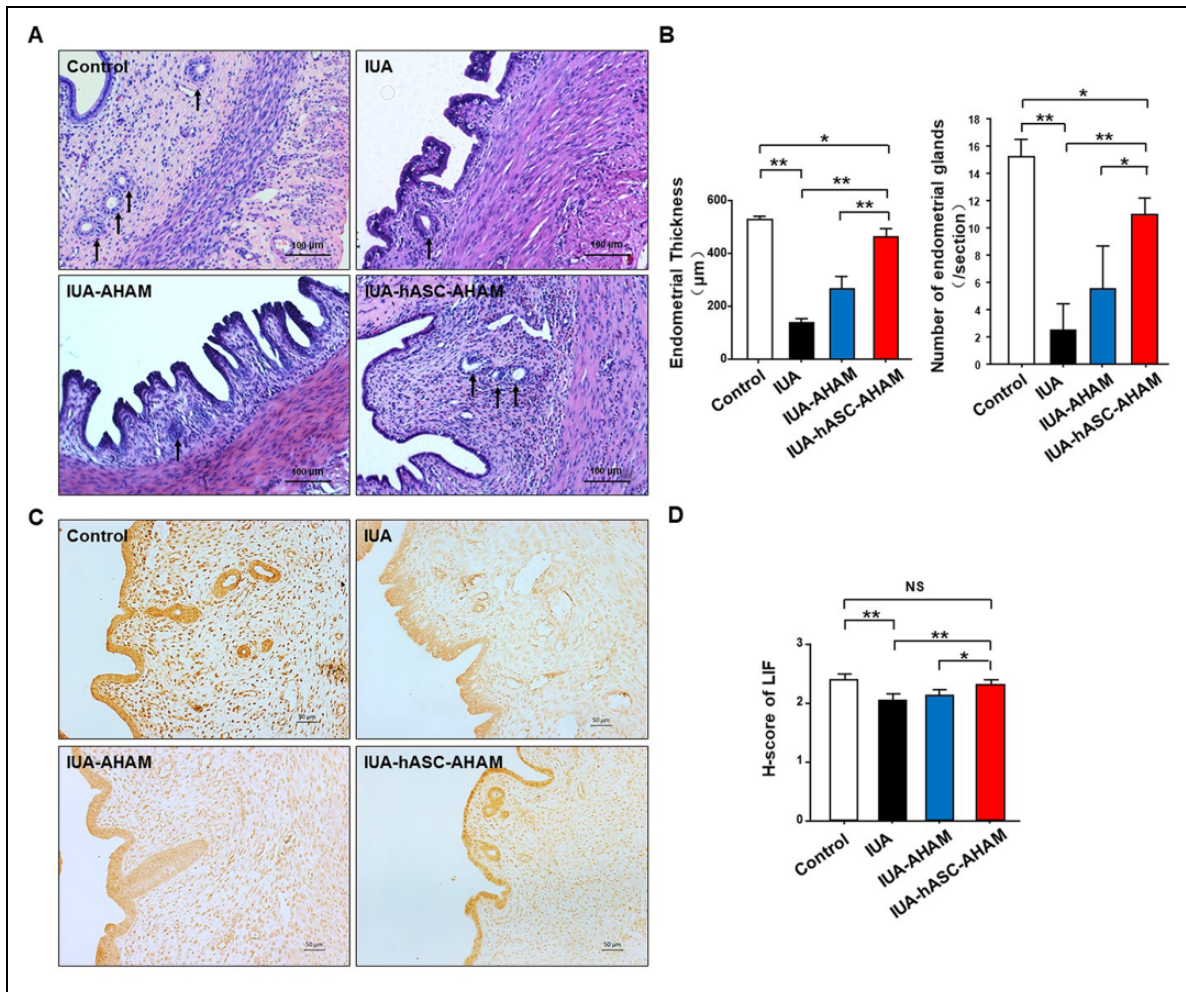


Figure 3. Histological analyses using H&E staining and LIF immunostaining. (A) The control, IUA, IUA-AHAM, and IUA-hASC-AHAM groups were analyzed by H&E staining. (B) The mean endometrial thickness and endometrial gland numbers in the four groups were quantitative analyzed. (C) Protein levels of LIF in the four groups were examined by immunohistochemical staining. (D) The LIF expression in the four groups was quantitative analyzed. NS: not significant, * $P < 0.05$, ** $P < 0.01$ by unpaired two-tailed Student's *t*-test. The data are presented as the means \pm SD. Black arrows indicate the glands. AHAM: acellular human amniotic membrane; hASC: human adipose stem cell; H&E: hematoxylin and eosin; IUA: intrauterine adhesion; IUA-AHAM: IUA treated with AHAM; IUA-hASC-AHAM: IUA treated with hASC-AHAM; LIF: leukemia inhibitory factor.

and ANG in hASCs; (ii) transplantation of the hASC-AHAM grafts can aid in the repair of injured endometrial tissue, resulting a thicker endometrium, increased gland numbers, increased receptivity of the endometrium, and higher vascular density; and (iii) hASCs in the injured endometrium can express VEGF and ANG, suggesting that hASC-AHAM grafts can promote endometrial repair through the expression of angiogenic factors. Thus, the transplantation of hASC-AHAM grafts offers an alternative approach to repair damaged endometrial tissue, and these results show the therapeutic potential of using auto hASCs derived from patient stem cells for treating IUA.

Asherman's syndrome is a condition characterized by the presence of IUA and/or fibrosis due to trauma to the basal layer of the endometrium. This syndrome may impact reproductive outcomes, causing infertility or recurrent

miscarriage. Hysteroscopy is now the gold standard for the diagnosis and treatment of IUAs, as this procedure separates the adhesions and restores the normal anatomy of the uterine cavity. However, the extent to which endometrial regeneration takes place will determine the surgical outcome and reproductive function. For moderate and severe IUA, the stroma of the endometrium is largely replaced by fibrous tissue, and glands are replaced by inactive cubocolumnar endometrial epithelium. In addition, the functional layer is replaced by an epithelial monolayer that is unresponsive to hormonal stimulation, such that the tissue is typically avascular overall. In such a situation, promoting endometrial repair remains challenging, primarily because IUA is a limiting step to the success of the surgery^{1,2}.

Stem cell therapy is a novel approach for treating tissue damage and promoting tissue regeneration. Compared to

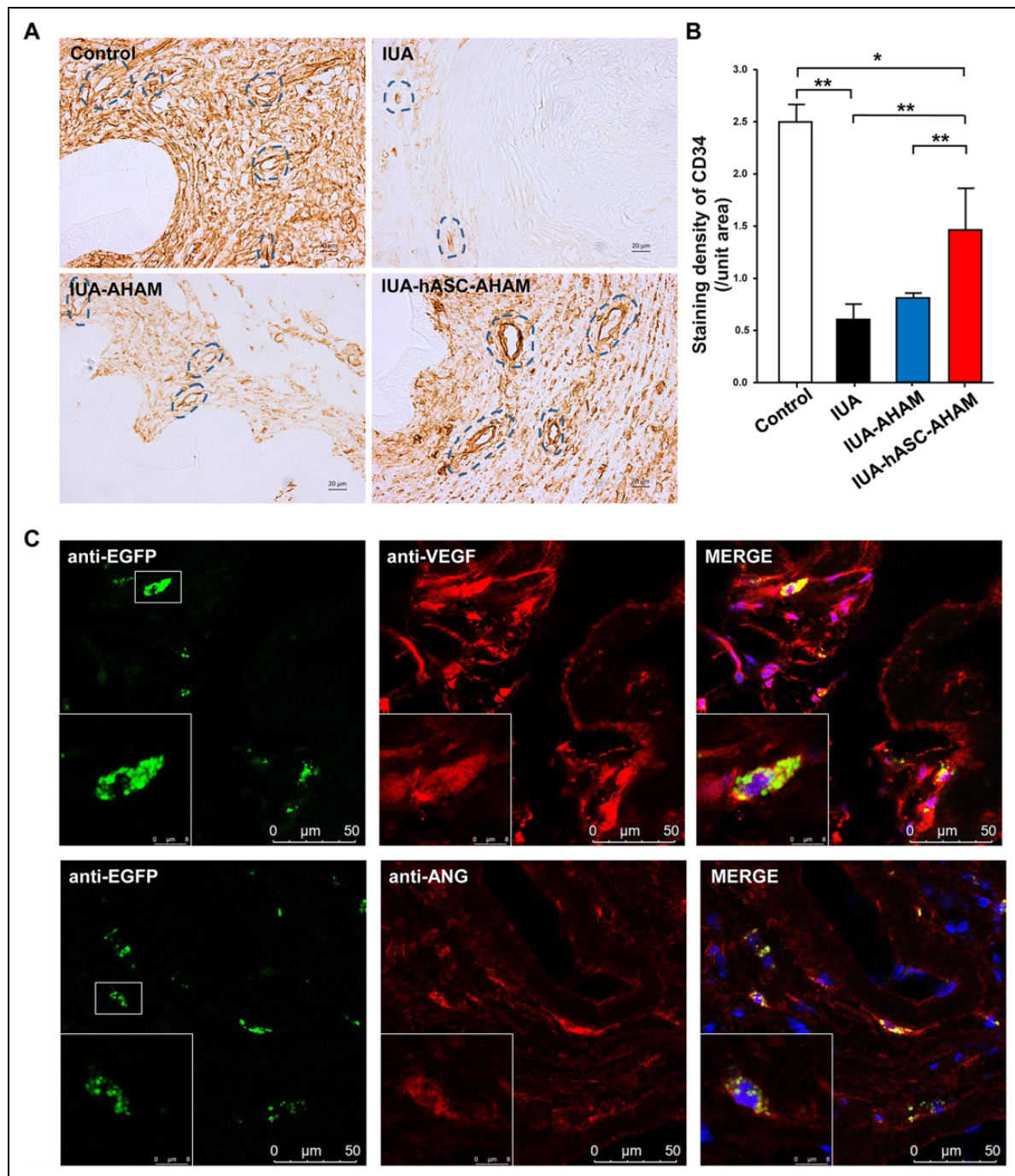


Figure 4. The expressions of CD34, VEGF, and ANG were analyzed via immunohistochemistry. (A) The expression of CD34 was analyzed via immunohistochemistry. Scale bars: 20 μm . (B) The staining densities of CD34 in the four groups were quantitative analyzed. (C) Protein levels of EGFP (green), VEGF, and ANG (red) in the hASC-AHAM group were determined by immunofluorescence staining. White boxes show the magnified areas. Blue circles indicate the vessels. AHAM: acellular human amniotic membrane; ANG: angiogenin; EGFP: enhanced green fluorescent protein; hASC: human adipose stem cell; IUA: intrauterine adhesion; IUA-AHAM: IUA treated with AHAM; IUA-hASC-AHAM: IUA treated with hASC-AHAM; VEGF: vascular endothelial growth factor.

other stem cell types, tissue-derived stem cells have many practical advantages in tissue engineering because these cells avoid the ethical issues of acquiring embryonic stem cells and the safety issues associated with tumor formation in

recipient patients. Compared with other tissues, adipose tissue is rich in source, easy to obtain, and can achieve autologous transplantation. Therefore, hASCs are the most promising source of stem cells for future use²².

Although studies have shown that stem cells can promote endometrial regeneration²³, the exact mechanism of this process remains unclear. It is known that there is vascular closure in the endometrial tissue in patients with IUA, and that angiogenesis occurs in the endometrium after treatment. Angiogenesis in the endometrial tissues is important and may affect endometrial repair²⁴. Furthermore, it has been reported that stem cells can change the internal environment of tissues through exosomes and promote tissue repair^{25,26}. In this study, hASC-AHAM grafts can promote the repair of endometrial damage in rats. After transplantation of hASC-AHAM, the endometrial vascular density of rats increased, and hASCs in the grafts expressed VEGF and ANG. Therefore, we believe that the hASC-AHAM graft increases the endometrial blood flow through expressing angiogenic factors by hASCs, thereby promoting endometrial repair.

At present, the main adjuvant therapies used to prevent adhesion recurrence after hysteroscopic adhesiolysis include using an intrauterine contraceptive device, an intrauterine balloon, a biodegradable gel, or a HAM, as surgical barriers to keep adjacent wound surfaces mechanically separated from one another²⁷. Since the late 1990s, the increasing potential of HAM as an adjuvant to prevent recurrence of adhesion reformation has been recognized. HAM is of low immunogenicity with no or minimal immune responding during transplantation. In addition, clinical studies have shown that the use of an amnion graft following intrauterine adhesiolysis appears to improve menstruation and reduce adhesion reformation recurrence by facilitating epithelialization, while reducing inflammation, scarring, and adhesion formation²⁷⁻²⁹. However, the transportation and preservation of fresh amniotic membrane is more difficult, so the application of fresh amniotic membrane has been restricted. Available evidence supports that viability of the tissue components of the amniotic membrane is not essential for its biological effectiveness. The amniotic membrane matrix contains various growth factors, proteases, and effective anti-inflammatory proteins, which makes amniotic membrane an important value in promoting epithelial formation, tissue healing, and inhibiting inflammation and fibrosis. Therefore, whether it contains epithelial cells has no significant difference in the efficacy of amniotic membrane. In fact, the decellularization process retains cytokines and maintains the original arrangement of collagen fibers. AHAM may retain its original function while reducing immunogenicity^{30,31}.

It appears from the results of our study that the combined use of stem cells and AHAM produced a synergistic beneficial effect in that the addition of the stem cells helps to improve endometrial regeneration, and the three-dimensional scaffolding provided by the AHAM results in an enhancement of the overall therapeutic potential of cells by improving the anti-inflammatory and angiogenic properties, stemness, and survival of stem cells after transplantation^{32,33}. In the present study, we chose to remove the maternal epithelial cells from HAM to generate an AHAM,

which may have lower immunogenicity and would be potentially more suitable as a graft.

In a sense, the model described in this study represents a stem cell sustained release system, using amniotic membrane as stem cells scaffold, and allowing the stem cells to continuously secrete angiogenesis factors to promote endometrial repair. Such an approach also negates the need to inject stem cells into the peripheral circulation with the hope that it will eventually enter the uterine cavity and help to ensure that the stem cells remain in the uterine cavity.

In this study, we also compared the expression of LIF between the four groups and showed that the IUA-hASC-AHAM group expressed more LIF than the injury group, while IUA-hASC-AHAM group expressed the same level of LIF as observed in the control group. LIF is a multifunctional biological cytokine that regulates the epithelial cell adhesive properties of the endometrium and is well recognized as a marker of endometrial receptivity^{34,35}. These findings are consistent with an improved endometrial function in the IUA-hASC-AHAM group.

Conclusion

In this study, the use of an AHAM as a three-dimensional scaffold combined with hASCs was shown to increase endometrial repair by promoting blood vessel regeneration. This finding provides the scientific basis for the potential use of these grafts in a novel individual therapeutic strategy for endometrial injury.

Author Contributions

XH, HZ, and EX conceived the study. XH, YM, XL, and WL performed laboratory analyses. XH wrote the draft. XH, HZ, and T-CL made a critical revision of the manuscript. All authors read and approved the final manuscript.

Ethical Approval

The study was approved by the Ethics Committee of Capital Medical University, Beijing, China (2015SY72 and AEEI-2017-105).

Statement of Human and Animal Rights

All experimental procedures involving human and animals were conducted in accordance with the Committee for Animal Care of Capital Medical University.

Statement of Informed Consent

We confirm that guidelines on patient consent have been met and any details of informed consent obtained are indicated within the text of the submitted manuscript.

Declaration of Conflicting Interests


The author(s) declared no potential conflicts of interest with respect to the research, authorship, and/or publication of this article.

Funding

The author(s) disclosed receipt of the following financial support for the research, authorship, and/or publication of this article: This

work was supported by the Project of excellent talent funding of Beijing Xicheng District (2017), the National Natural Science Foundation of China (grant number 81770616), and the Beijing Municipal Natural Science Foundation (grant number 5172009).

ORCID iD

Xiaowu Huang  <https://orcid.org/0000-0003-1611-3088>

Supplemental Material

Supplemental material for this article is available online.

References

1. Yu D, Wong YM, Cheong Y, Xia E, Li TC. Asherman syndrome—one century later. *Fertil Steril*. 2008;89(4):759–779.
2. Garcia-Velasco JA, Acevedo B, Alvarez C, Alvarez M, Bellver J, Fontes J, Landeras J, Manau D, Martinez F, Muñoz E, Robles A, et al. Strategies to manage refractory endometrium: state of the art in 2016. *Reprod Biomed Online*. 2016;32(5):474–489.
3. Nadig RR. Stem cell therapy - Hype or hope? A review. *J Conserv Dent*. 2009;12(4):131–138.
4. Chan RW, Schwab KE, Gargett CE. Clonogenicity of human endometrial epithelial and stromal cells. *Biol Reprod*. 2004;70(6):1738–1750.
5. Gargett CE, Schwab KE, Deane JA. Endometrial stem/progenitor cells: the first 10 years. *Hum Reprod Update*. 2016;22(2):137–163.
6. Deane JA, Gualano RC, Gargett CE. Regenerating endometrium from stem/progenitor cells: is it abnormal in endometriosis, Asherman's syndrome and infertility? *Curr Opin Obstet Gynecol*. 2013;25(3):193–200.
7. Song T, Zhao X, Sun H, Li X, Lin N, Ding L, Dai J, Hu Y. Regeneration of uterine horns in rats using collagen scaffolds loaded with human embryonic stem cell-derived endometrium-like cells. *Tissue Eng Part A*. 2015;21(1–2):353–361.
8. Azizi R, Aghebatimaleki L, Nouri M, Marofi F, Negargar S, Yousefi M. Stem cell therapy in Asherman syndrome and thin endometrium: stem cell-based therapy. *Biomed Pharmacother*. 2018;102:333–343.
9. Lee YJ, Yi KW. Bone marrow-derived stem cells contribute to regeneration of the endometrium. *Clin Exp Reprod Med*. 2018;45(4):149–153.
10. Zhang L, Li Y, Guan CY, Tian S, Xia HF. Therapeutic effect of human umbilical cord-derived mesenchymal stem cells on injured rat endometrium during its chronic phase. *Stem Cell Res Ther*. 2018;9(1):36–50.
11. Hu J, Song K, Zhang J, Zhang Y, Tan BZ. Effects of menstrual blood-derived stem cells on endometrial injury repair. *Mol Med Rep*. 2019;19(2):813–820.
12. Domina A, Novikova P, Obidina J, Fridlyanskaya I, Alekseenko L, Kozhukharova I, Lyublinskaya O, Zenin V, Nikolsky N. Human mesenchymal stem cells in spheroids improve fertility in model animals with damaged endometrium. *Stem Cell Res Ther*. 2018;9(1):50–61.
13. Shao X, Ai G, Wang L, Qin J, Li Y, Jiang H, Zhang T, Zhou L, Gao Z, Cheng J, Cheng Z. Adipose-derived stem cells transplantation improves endometrial injury repair. *Zygote*. 2019;27(6):367–374.
14. Hunter RK, Nevitt CD, Gaskins JT, Keller BB, Bohler HCL, Leblanc AJ. Adipose-derived stromal vascular fraction cell effects on a rodent model of thin endometrium. *PLoS One*. 2015;10(12):e0144823.
15. Mahmoudifar N, Doran PM. Mesenchymal stem cells derived from human adipose tissue. *Methods Mol Biol*. 2015;1340:53–64.
16. Rahmati M, Pennisi CP, Mobasheri A, Mozafari M. Bioengineered scaffolds for stem cell applications in tissue engineering and regenerative medicine. *Adv Exp Med Biol*. 2018;1107:73–89.
17. Yuan J, Li W, Huang J, Guo X, Li X, Lu X, Huang X, Zhang H. Transplantation of human adipose stem cell-derived hepatocyte-like cells with restricted localization to liver using acellular amniotic membrane. *Stem Cell Res Ther*. 2015;6:217–230.
18. Li X, Yuan J, Li W, Liu S, Hua M, Lu X, Zhang H. Direct differentiation of homogeneous human adipose stem cells into functional hepatocytes by mimicking liver embryogenesis. *J Cell Physiol*. 2014;229(6):801–812.
19. Gao H, Zhao Y, Li P. Establishment and identification of rat thin endometrium model. *Life Sci Res*. 2011;15:426–431.
20. Han H, Gai X, Tian F, Yan P, Wang XN. Establishment and evaluation of rat model of endometrial injury. *Chin J Reprod Contracep*. 2017;37:33–37.
21. Lu X, Yuan J, Guo XY, Li WH, Shang HW, Zhang LX, Huang XH, Zhang HY. Preparation for acellular human amniotic membrane matrix and assessment the immunogenic property. *Acta Anatomica Sinica*. 2016;47(4):557–562.
22. Zhu Y, Liu T, Song K, Fan X, Ma X, Cui Z. Adipose-derived stem cell: a better stem cell than BMSC. *Cell Biochem Funct*. 2008;26(6):664–675.
23. Gargett CE, Ye L. Endometrial reconstruction from stem cells. *Fertil Steril*. 2012;98(1):11–20.
24. Chen Y, Chang Y, Yao S. Role of angiogenesis in endometrial repair of patients with severe intrauterine adhesion. *Int J Clin Exp Pathol*. 2013;6(7):1343–1350.
25. Shabbir A, Cox A, Rodriguezmenocal L, Salgado M, Van Badiavas E. Mesenchymal stem cell exosomes induce proliferation and migration of normal and chronic wound fibroblasts, and enhance angiogenesis *in vitro*. *Stem Cells Dev*. 2015;24(14):1635–1647.
26. Teng X, Chen L, Chen W, Yang J, Yang Z, Shen Z. Mesenchymal stem cell-derived exosomes improve the microenvironment of infarcted myocardium contributing to angiogenesis and anti-inflammation. *Cell Physiol Biochem*. 2015;37(6):2415–2424.
27. Bosteels J, Weyers S, Kasius J, Torrance H, Broekmans FJ, Chua SJ, Mol BWJ. Anti-adhesion therapy following operative hysteroscopy for treatment of female subfertility. *Cochrane Database Syst Rev*. 2017;11(11):CD011110.
28. Zheng F, Zhu B, Liu Y, Wang R, Cui Y. Meta-analysis of the use of amniotic membrane to prevent recurrence of intrauterine

- adhesion after hysteroscopic adhesiolysis. *Int J Gynaecol Obstet.* 2018;143(2):145–149.
29. Peng X, Li T, Zhao Y, Guo Y, Xia E. Safety and efficacy of amnion graft in preventing reformation of intrauterine adhesions. *J Minim Invasive Gynecol.* 2017;24(7):1204–1210.
 30. Amer MI, Abd-El-Maeboud KH, Abdelfatah I, Salama FA, Abdallah AS. Human amnion as a temporary biologic barrier after hysteroscopic lysis of severe intrauterine adhesions: pilot study. *J Minim Invasive Gynecol.* 2010;17(5):605–611.
 31. Jorge LF, Francisco JC, Bergonse N, Baena C, Carvalho K, Abdelwahid E, Neto J, Moreira L, Guarita-Souza LC. Tracheal repair with acellular human amniotic membrane in a rabbit model. *J Tissue Eng Regen Med.* 2018;12(3):e1525–e1530.
 32. Petrenko Y, Syková E, Kubinová Š. The therapeutic potential of three-dimensional multipotent mesenchymal stromal cell spheroids. *Stem Cell Res Ther.* 2017;8:94–102.
 33. Clark K, Janorkar AV. Milieu for endothelial differentiation of human adipose-derived stem cells. *Bioengineering (Basel).* 2018;5(4):82–91.
 34. Camargo-Díaz F, García V, Ocampo-Bárceñas A, González-Marquez H, López-Bayghen E. Colony stimulating factor-1 and leukemia inhibitor factor expression from current-cycle cannula isolated endometrial cells are associated with increased endometrial receptivity and pregnancy. *BMC Womens Health.* 2017;17:63–69.
 35. Shuya LL, Menkhorst EM, Yap J, Li P, Lane N, Dimitriadis E. Leukemia inhibitory factor enhances endometrial stromal cell decidualization in humans and mice. *PLoS One.* 2011;6(9):e25288.